Structural and electronic properties of the 17 K superconductor $Sr_2ScFePO_3$ in comparison to $Sr_2ScFeAsO_3$ from first principles calculations

I. R. Shein* and A. L. Ivanovskii

Institute of Solid State Chemistry, Ural Branch, Russian Academy of Sciences, 91, Pervomaiskaya ul., Ekaterinburg 620990, Russia

(Received 28 March 2009; revised manuscript received 5 May 2009; published 15 June 2009)

The results of *ab initio* full-potential method with mixed basis APW+lo-generalized gradient approximation calculations of the band structure of the recently synthesized tetragonal (space group $P4/nmm$) layered iron-phosphide oxide 17 K superconductor $Sr_2ScFePO_3$ are presented in comparison with the hypothetical isostructural iron-arsenide-oxide phase $Sr_2ScFeAsO_3$. For these phases, the optimized structural data, energy bands, total and partial densities of states, Fermi-surface topology, low-temperature electron specific heat, and molar Pauli paramagnetic susceptibility have been obtained and discussed in comparison with available experiments with hypothetical and related layered FeAs and FeP superconductors.

DOI: 10.1103/PhysRevB.79.245115 PACS number(s): 74.25.Jb, 71.20.−b, 74.70.−b

I. INTRODUCTION

The recent discovery of superconductivity at T_c's to 55–56 K in the layered iron-pnictide systems[1–5] has sparked enormous interest in this class of materials and led to an intensive search for related superconductors (SCs). As a result, at least five groups of such materials have been discovered to date: (i) the group of oxygen-containing "1111" phases based on the layered arsenide oxides *Ln*FeAsO (*Ln*=La, Ce,…,Gd, Tb, Dy); (ii) the related oxygen-free 1111 phases (for example, *Ln*FeAsF); (iii) the group of three-component layered "122" SCs based on AFe_2As_2 phases (*A*=Sr, Ba); (iv) the so-called "111" SCs (LiFeAs and NaFeAs); (v) layered phases in binary Fe-Se(Te) systems. Besides, a lot of related systems with various pnictogens (*Pn*=P, Sb, Bi) or transition metals which replace Fe (*TM*=Cr, Co, Ni, Ru, Rh, Ir, etc.) have been synthesized and examined; see reviews.[6,7]

All the mentioned materials are anisotropic (quasi-two-dimensional) systems with a crystal structure formed by negatively charged blocks $[TM_2Pn_2]^{\delta-}$ alternating with positively charged blocks or atomic sheets. The superconductivity in all these systems is attributed to the $[TM_2Pn_2]$ blocks which make a decisive contribution to the near-Fermi region of these materials, while the positively charged blocks (for example, $[LnO]^{\delta+}$ or $A^{\delta+}$) serve as the so-called charge reservoirs.[1–7]

The available data[1–7] make it possible to note[8] an interesting empirical correlation between the space separation of the conducting [FeAs] blocks in the FeAs superconductors and their critical temperatures T_c's. For example, the maximum T_c's (about 55–56 K) have been reached to date for doped 1111 phases $Gd_{1-x}Th_yFeAsO$ (Ref. 2) and $SmFeAsO_{1-x}F_x$.[9] In these materials, the distances l between the neighboring [FeAs]/[FeAs] blocks separated by $[LnO]^{\delta+}$ blocks are about 8.7 Å. For the 122 phases where the neighboring [FeAs]/[FeAs] blocks are separated by monatomic sheets of alkali-earth metals ($l\sim6.5$ Å), the T_c's are reduced to 38 K. Even lower T_c's ~18 K were revealed for the 111 phases where the [FeAs]/[FeAs] blocks are separated by alkali-metal sheets ($l\sim6.4$ Å). Let us also mention the related iron-containing SC FeSe with a tetragonal structure (anti-PbO type) and directly contacting [FeSe]/[FeSe] blocks, for which T_c under normal conditions does not exceed 7–8 K.[10] The nature of this correlation is still unclear. One of the possible explanations[8] is based on the hypothesis (see Refs. 6 and 7) that spin fluctuations are important in the superconductivity mechanism of the FeAs materials when the increasing space separation of the superconducting [FeAs]/[FeAs] blocks hinders the formation of long-range antiferromagnetic order and thus promotes an increase in T_c's.

As compared with FeAs SCs, their isostructural FeP analogs show much smaller T_c's which usually do not surpass 10 K. Some explanations of the occurrence of the low-temperature superconductivity in iron-phosphide SCs (the role of interatomic Fe-*Pn* distances, the absence of long-range magnetic order, some peculiarities of the near-Fermi bands, etc.) were discussed recently.[6,7,11–19]

In view of these circumstances the recent discovery[20–28] of a new family of the so-called "21113" five-component phases: $Sr_2MFeAsO_3$ (*M*=Sc, Ti, V, Cr, Co), $Ba_2ScFeAsO_3$, $Ca_2ScFeAsO_3$, $Sr_2ScFePO_3$, $Sr_2ScCoAsO_3$, $Sr_2ScFePO_3$, $Sr_2ScNiPO_3$, and $Sr_2ScNiAsO_3$ seems to be very interesting. Now it is possible to give a preliminary summary of their most remarkable features.

(1) These systems adopt an alternating stacking of $[M'Pn]$ (M'=Fe, Co, Ni and *Pn*=As or P) and perovskite-type $[A_2MO_3]$ blocks (*A*=Ca, Sr, Ba and *M*=Sc, Ti, V, Cr), where $[M'Pn]/[M'Pn]$ separation ($l\sim15.5$ Å) is the longest among all known Fe-based SCs.

(2) The above blocks $[M'Pn]$ are separated by perovskite-type blocks $[A_2MO_3]$ which contain transition *d* metals (*M*=Sc, Ti, V, Cr) while all earlier known FeAs phases (such as LaFeAsO, $BaFe_2As_2$, or LiFeAs, etc.) contain only the atoms of alkaline, alkaline-earth, or rare-earth metals in these blocks.

(3) The majority of earlier known FeAs parent phases are nonsuperconducting and lie on the border of their structural and magnetic instability, whereas superconductivity arises as a result of hole or electron doping. In turn, doping is usually achieved by various atomic replacements, such as (a) replacements of *Ln* and *A* atoms inside insulating blocks by other *Ln* and *A* atoms; (b) replacements of oxygen atoms inside insulating blocks by other *p* nonmetal atoms; (c) re-

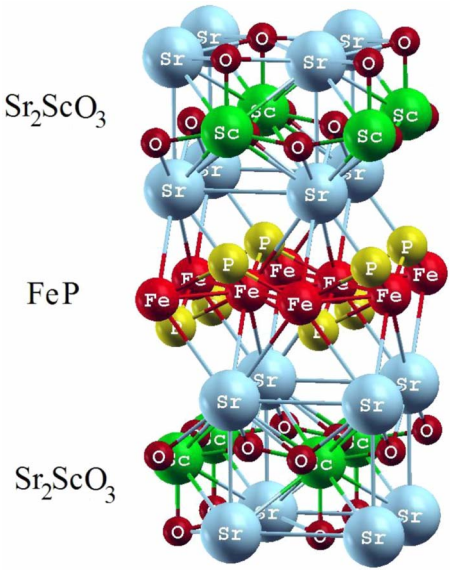

FIG. 1. (Color online) Crystal structure of the phase $Sr_2ScFePO_3$ (space group $P4/nmm$). The main building blocks [FeP] and [Sr_2ScO_3] are shown.

placements of Fe atoms by magnetic ($3d$:Mn, Co, Ni) or nonmagnetic ($4d$, $5d$:Ru, Rh, Ir, etc.) metal atoms inside [FeAs] blocks; (d) replacements of As atoms inside [FeAs] blocks by other pnictogens, see Refs. 6 and 7. However, according to the recent data[21,28] partial substitution of Ti for Sc or Ti for Cr in blocks [Sr_2MO_3] leads to the appearance of superconductivity for some of 21113 systems. This situation differs drastically from the known picture for all other FeAs systems. Thus, for 21113 phases, partial replacement of d metals in blocks [Sr_2MO_3] should be considered as an unusual type of doping, which was not used earlier.

(4) Finally, among the discovered 21113 systems[20–28] there are at least two unusual phases. Namely, the five-component iron-phosphide-oxide phase $Sr_2ScFePO_3$ with $T_c \sim 17$ K (Ref. 27) which is the highest transition temperature among all arsenic-free iron-based systems, and $Sr_2CrFeAsO_3$ with $T_c \sim 37$ K (Ref. 24) which is the highest transition temperature among all undoped FeAs systems.

Thus, today it is possible to assert that a new group of 21113 systems[20–28] is discovered and this family proposed new guidelines for the development of superconducting materials. In this context, we present here a detailed *ab initio* study of two prototype (As-containing and P-containing) phases for the new family of 21113 systems: $Sr_2ScFePO_3$ and $Sr_2ScFeAsO_3$. We focus our attention on their structural, electronic properties, and the Fermi-surface topology. As a result, the optimized structural data, energy bands, total and partial densities of states, Fermi-surface topology, low-temperature electron specific heat, and molar Pauli paramagnetic susceptibility have been determined for $Sr_2ScFePO_3$ and $Sr_2ScFeAsO_3$ (termed further P21113 and As21113) and compared with available experiments and related layered FeAs and FeP superconductors.

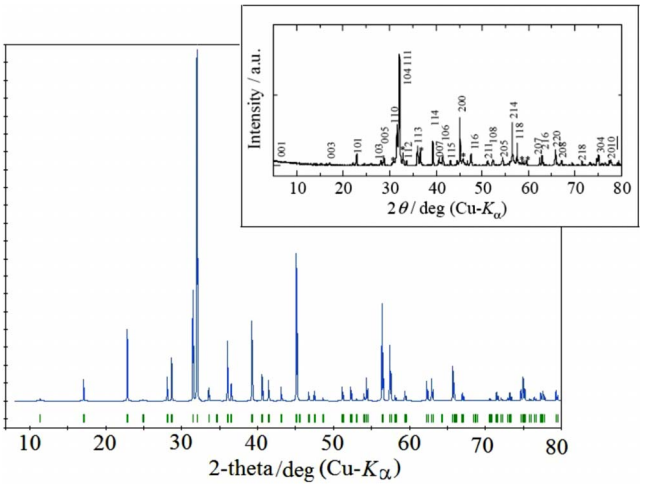

FIG. 2. (Color online) Calculated theoretical XRD pattern of the $Sr_2ScFePO_3$ phase as compared with the powder XRD pattern (Ref. 20) (in the inset).

II. COMPUTATIONAL METHOD AND MODELS

Our calculations were carried out by means of the full-potential method with mixed basis APW+lo (FLAPW) implemented in the WIEN2K suite of programs.[29] The generalized gradient approximation (GGA) to exchange-correlation potential in the PBE form[30] was used. The plane-wave expansion was taken up to $R_{MT} \times K_{MAX}$ equal to 7, and the k sampling with $13 \times 13 \times 5$ k points in the Brillouin zone was used. The calculations were performed with full-

TABLE I. The optimized atomic positions for $Sr_2ScFePO_3$ and $Sr_2ScFeAsO_3$.

System	$Sr_2ScFePO_3$			$Sr_2ScFeAsO_3$		
Atomic positions	x	y	z	x	y	z [a]
$Sr_1(2c)$	0.25	0.25	0.3232	0.25	0.25	0.3176 (0.3113)
$Sr_2(2c)$	0.25	0.25	0.0878	0.25	0.25	0.0870 (0.0847)
$Sc(2c)$	0.25	0.25	0.8024	0.25	0.25	0.8042 (0.8071)
$O_1(4f)$	0.75	0.25	0.2213	0.75	0.25	0.2179 (0.2143)
$O_2(2c)$	0.25	0.25	0.9319	0.25	0.25	0.9325 (0.9301)
$Fe(2b)$	0.75	0.25	0.5	0.75	0.25	0.5 (0.5)
$P(As)(2c)$	0.25	0.25	0.5673	0.25	0.25	0.5778 (0.5854)

[a]In parentheses the available experimental data (Ref. 20) are given with displacement on $c/2$.

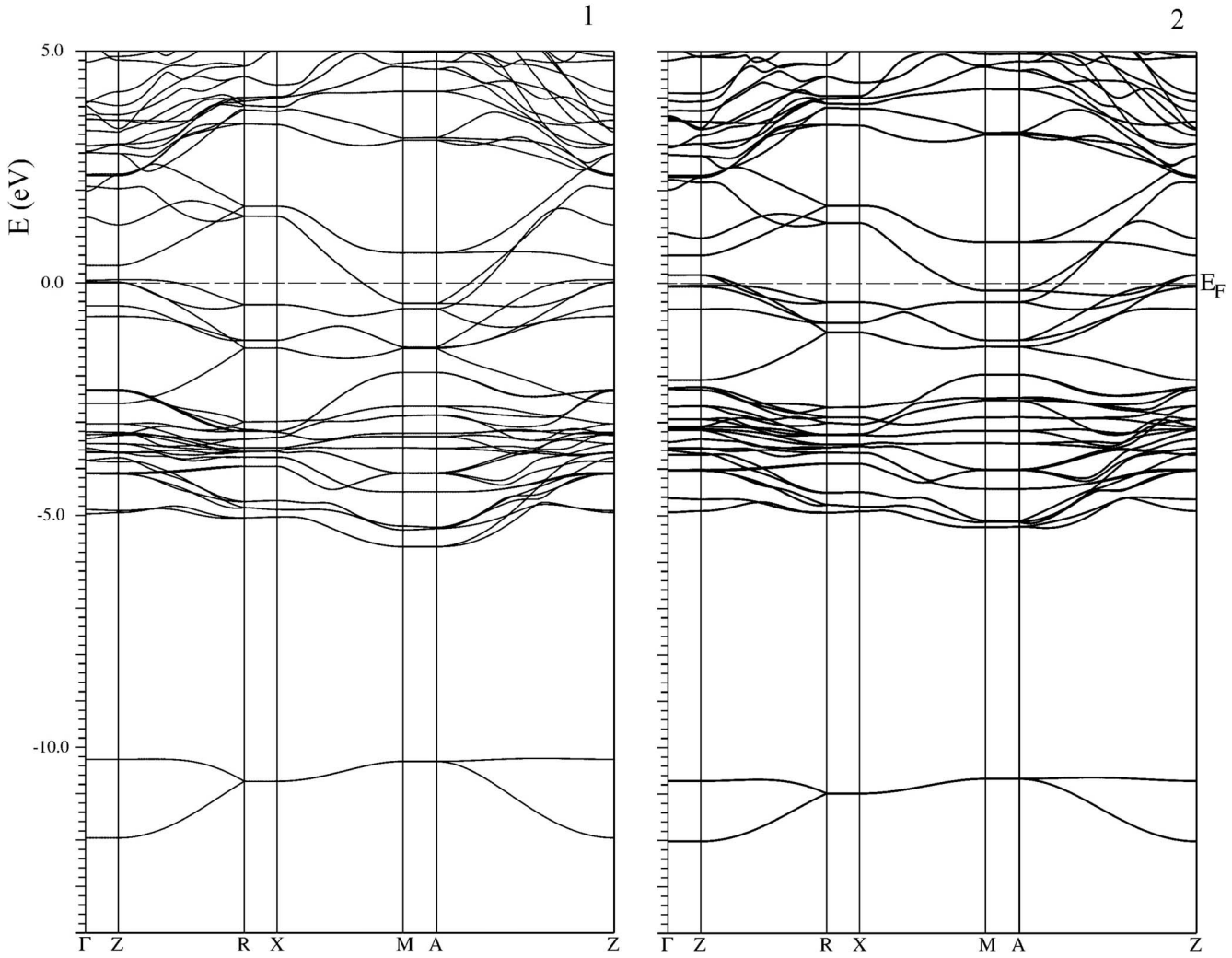

FIG. 3. Electronic bands for (1) $Sr_2ScFePO_3$ and (2) $Sr_2ScFeAsO_3$.

lattice optimizations including the atomic positions. The self-consistent calculations were considered to be converged when the difference in the total energy of the crystal did not exceed 0.1 mRy and the difference in the total electronic charge did not exceed $0.001e$ as calculated at consecutive steps. The hybridization effects were analyzed using the densities of states (DOSs), which were obtained by the modified tetrahedron method[31] and some peculiarities of intra-atomic bonding picture were visualized by means of charge-density maps.

III. RESULTS AND DISCUSSION

A. Structural properties

The newly synthesized $Sr_2ScFePO_3$ adopts a complicated tetragonal (space group $P4/nmm$) crystal structure; the experimentally obtained lattice constants are $a=4.016$ Å and $c=15.543$ Å.[27] This material consists of stacking of antifluorite [FeP] blocks and perovskite-type $[Sr_2ScO_3]$ blocks as depicted in Fig. 1. As no detailed atomic coordinates are reported for the P21113 phase,[27] at the first stage the full structural optimization of this phase was performed both over the lattice parameters and the atomic positions (see Table I).

The calculated theoretical x-ray diffraction (XRD) pattern of the P21113 phase coincides well with powder XRD data,[27] see Fig. 2. Besides, the calculated lattice constants for P21113 ($a^{calc}=4.008$ Å and $c^{calc}=15.444$ Å) are in reasonable agreement with the available[27] experiment: the divergences $(a^{calc}-a^{exp})/a^{exp}$ and $(c^{calc}-c^{exp})/c^{exp}$ are −0.002 and −0.006, respectively, and should be attributed probably to the presence of a certain amount (~10%) of the secondary phase $SrFe_2P_2$ in the synthesized samples.[27] According to our calculations, the Fe-P-Fe angles are 77.7° and 125° and the Fe-Fe and Fe-P distances are 2.824 Å and 2.251 Å, respectively. The corresponding experimental values[27] are 74.8°, 118°, and 2.840 Å (Fe-Fe distances).

The same calculations were performed for the isostructural As21113. The calculated lattice constants ($a^{calc}=4.036$ Å and $c^{calc}=15.534$ Å) are in reasonable agreement with the available experiments ($a^{exp}=4.050$ Å, $c^{exp}=15.809$ Å in Ref. 20 and $a^{exp}=4.045$ Å, $c^{exp}=15.802$ Å in Ref. 22), as well as the atomic positions, see Table I. Note that the lattice constants for As21113 are greater than those for P21113—as should be expected when small phosphorus

TABLE II. Calculated bandwidths (in eV) of occupied states for $Sr_2ScFePO_3$ and $Sr_2ScFeAsO_3$.

System	$Sr_2ScFePO_3$	$Sr_2ScFeAsO_3$
Valence band (to E_F)	5.8	5.3
Band gap	4.5	5.5
Quasicore pnictogen *s* band	1.6	1.3

atoms (with the atomic radius $R^{at}=1.30$ Å) are replaced by larger arsenic atoms ($R^{at}=1.48$ Å) and simultaneous growth of Fe-Fe (2.85 Å) and Fe-As (2.35 Å) distances occurs.

At the same time our results show that the replacement P→As leads to some *anisotropic deformations* of the crystal structure caused by strong anisotropy of interatomic bonds; see also Refs. 16 and 32. Really, in comparison with P21113, a^{calc} for As21113 increases by about 0.05 Å versus c^{calc}, which increases by about 0.09 Å. Besides, the [FeAs] blocks are thicker than the [FeP] blocks, whereas the $[Sr_2ScO_3]$ blocks in As21113 are compressed as compared with those in P21113—for example, the Sr-Sr distances (between strontium atoms on the opposite sites of blocks $[Sr_2ScO_3]$) for As21113 are 3.58 Å—versus 3.64 Å for P21113. Note also that the calculated Fe-As-Fe angles (74.7° and 118.2°) for As42226 as compared to those of P21113 are more close to the ideal tetrahedron angles (109.5°), which is a factor favorable for superconductivity.[27,32,33]

B. Electronic band structure and Fermi surface

Figure 3 shows the band structure of P21113 and As21113 with optimized geometry as calculated along the high-symmetry *k* lines. For P21113, the occupied bands form three main groups in the intervals −11.9 to −10.3 eV, −5.8 to −1.4 eV, and from −1.4 eV to E_F. The Fermi level is crossed by low-dispersive bands mainly of the Fe 3*d* character; these bands form two electron pockets centered at *M* and three hole pockets centered at Γ. Note that a similar picture of the low-energy band structure (where the bands which cross the Fermi level have mainly the Fe $d_{xy,xz,yz}$ symmetry) was established for LaFeAsO (Refs. 6, 7, 34, and 35) whereas a significant difference between P21113 and the related low-temperature SC ($T_c\sim 2-5$ K) LaFePO (Refs. 12 and 34) comes from the third pocket (formed basically by the Fe $d_{3z^2-r^2}$ band) centered for the latter compound along the Γ→*Z* direction.

This difference in the low-energy band structure is mainly due to its great sensitivity to the interatomic distances and bonding angles in [Fe *Pn*] blocks, when these parameters for P21113 are more similar to those for LaFeAsO than to those for LaFePO; see also Ref. 27. Note that the low-energy Fe 3*d*-like bands for the recently synthesized[8] nonsuperconducting phase $(Sr_3Sc_2O_5)Fe_2As_2$ (where the conducting [FeAs]/[FeAs] blocks are also spaced by a very long distance $l\sim 13.4$ Å) are higher (over the Fermi level[36]) than for P21113, and this fact may be related to the absence of superconductivity for the ideal $(Sr_3Sc_2O_5)Fe_2As_2$, which probably will become a SC as a result of electron doping. Comparison of the data for P21113 and As21113 (Fig. 3) shows that these phases preserve the common features of their band structures; the obvious difference is the width and composition of the main band groups, see Table II.

The Fermi surface (FS) of P21113 is made of five sheets (five bands are crossing the Fermi level as shown in Fig. 4), which are cylindrical-like and parallel to the k_z direction. Three of them are holelike and are centered along the Γ-*Z* direction while two others (electroniclike) are centered along the A-M direction.

For As21113, the FS is made of four cylindrical-like sheets, among them two sheets centered along the Γ-*Z* direction are holelike while the others (electroniclike) are centered along the A-M line. All sheets are parallel to the k_z direction. As compared with the FS of P21113, the FS sheets for As21113 are "compressed."

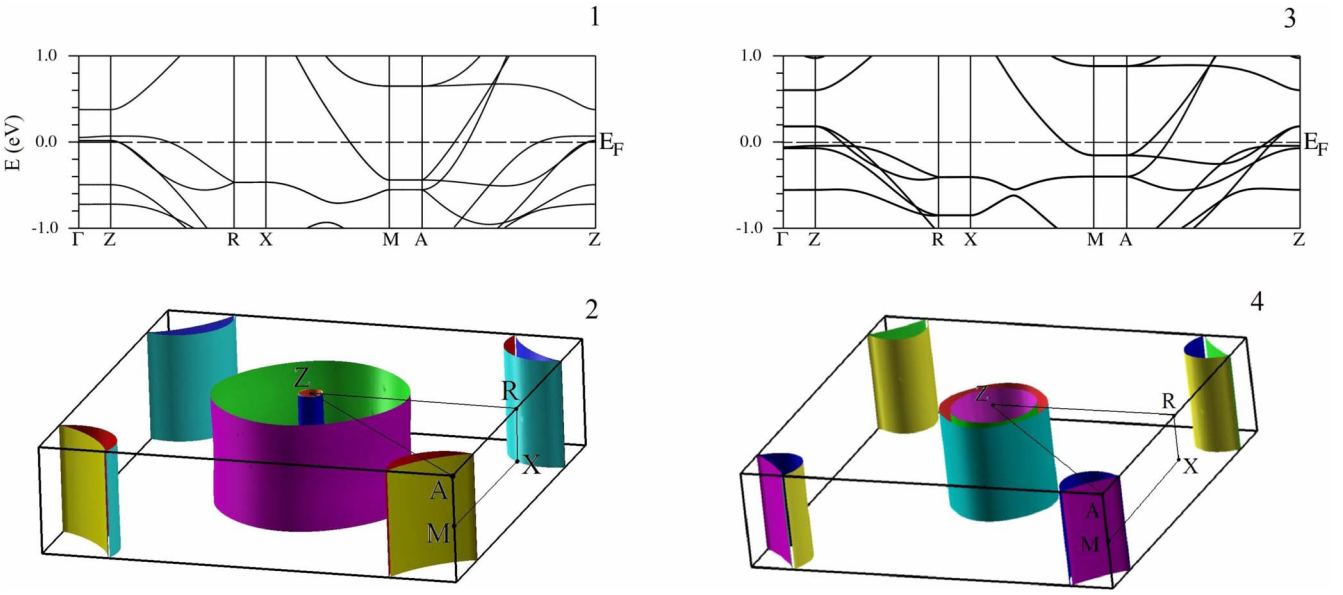

FIG. 4. (Color online) The near-Fermi bands and Fermi surfaces for $Sr_2ScFePO_3$ (1,2) and $Sr_2ScFeAsO_3$ (3,4).

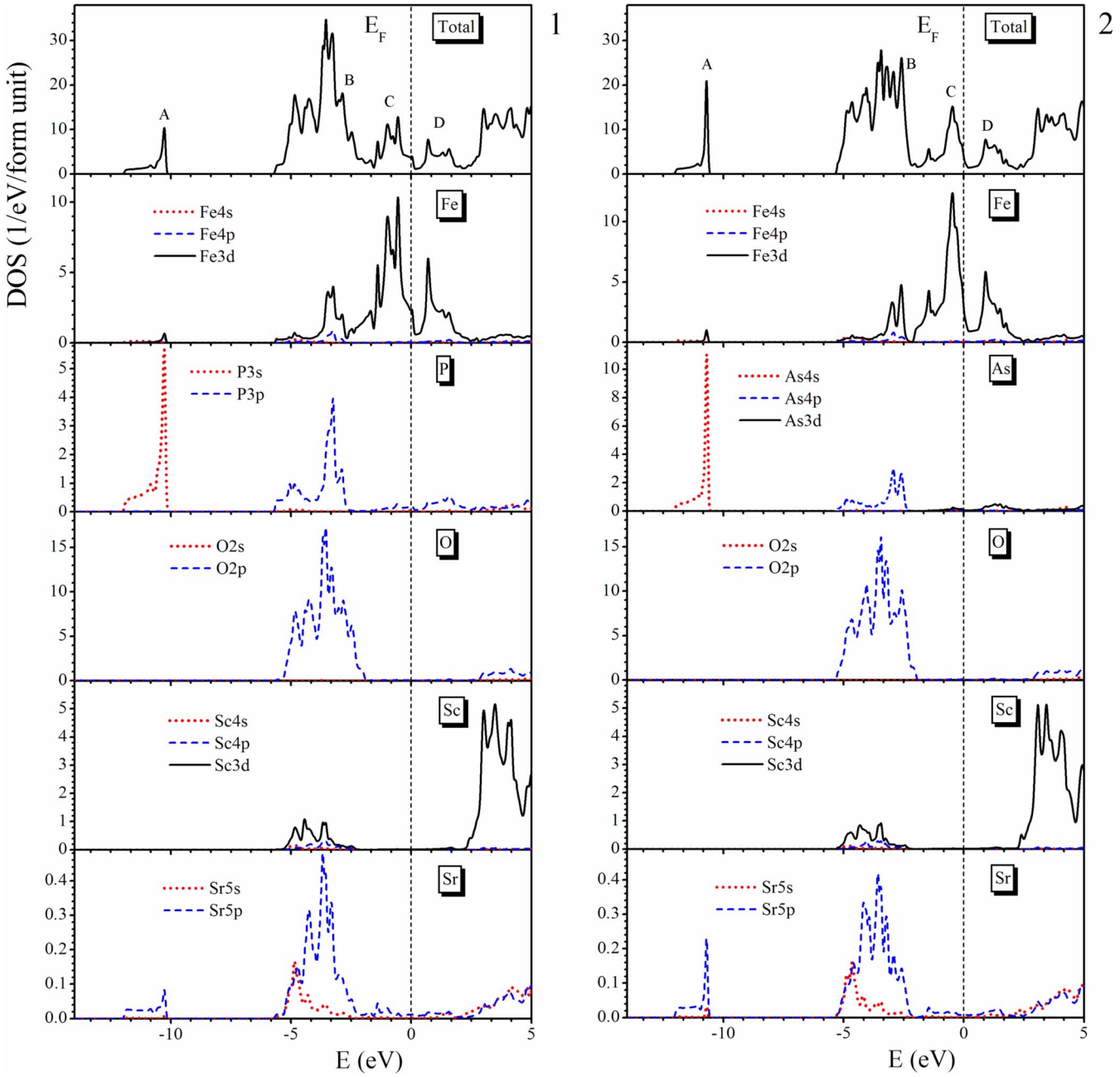

FIG. 5. (Color online) Total (upper panels) and partial densities of states (bottom panels) for (1) $Sr_2ScFePO_3$ and (2) $Sr_2ScFeAsO_3$.

C. Density of states

For further description of the electronic spectra of P21113 and As21113 we have plotted in Fig. 5 the total and partial DOSs. For P21113, at high binding energies (in the interval from −11.9 to −10.3 eV), the DOS peak A is almost completely made of P 3*s* orbitals with a very small admixture of Sr 5*p* orbitals. It is worth noting that the contributions from the valence *s*,*p* states of Sr to all the occupied bands are quite negligible, i.e., in P21113 (as well as in As21113) these atoms are in the form of cations close to Sr^{2+}.

In the next interval from −5.8 to −1.4 eV (peak B), all the atoms of the P21113 phase contribute to the DOS and these states are responsible for the hybridization effects, i.e., for interatomic covalent bonding. Taking into account the distribution of the corresponding atoms over the [FeP] and $[Sr_2ScO_3]$ blocks (see Fig. 1) it is seen that the formation of the Fe-P and Sc-O covalent bonds is due to the hybridization of Fe 3*d*-P 3*p* and Sc 3*d*-O 2*p* states, respectively, see also below. For As21113, the DOS peak A with high binding energies is mainly of the As 4*s* character, whereas the states in the interval from −5.3 to −2.1 eV (peak B) form the Fe-As and Sc-O bonds owing to hybridization of Fe 3*d*-As 4*p* and Sc 3*d*-O 2*p* states.

The occupied bands near the Fermi level (peaks C, Fig. 5) and the lower conduction bands (peaks D) in P21113 and As21113 are formed exclusively by the states of [FeP] and [FeAs] blocks, respectively. Therefore, the conduction in these phases is expected to be strongly anisotropic, i.e., hap-

TABLE III. Total and partial densities of states at the Fermi level (in states/eV f.u.), electronic heat capacity γ (in mJ K^{-2} mol^{-1}) and molar Pauli paramagnetic susceptibility χ (in 10^{-4} emu/mol) for $Sr_2ScFePO_3$ and $Sr_2ScFeAsO_3$.

System	$N^{\mathrm{Fe}\ 3d}(E_F)$	$N^{(\mathrm{P,As})p}(E_F)$	$N^{\mathrm{tot}}(E_F)$	γ	χ
$Sr_2ScFePO_3$	2.378	0.209	3.954	9.32	1.27
$Sr_2ScFeAsO_3$	2.779	0.081	3.754	8.85	1.21

pening mainly in these blocks. Notice that the contributions from P (As) states are much smaller than the contributions from Fe 3*d* orbitals, see Table III, where the total and orbital decomposed partial DOSs at the Fermi level, $N(E_F)$, are shown.

For As21113 the $N(E_F)$ value is about 5% lower than for P21113. This effect may be attributed mainly to the lowering of the contributions of As states to $N(E_F)$ whereas the density of Fe 3*d* states at the Fermi level increases by about 17%, Table III. Note also that for P21113 the Fermi level is located on a flat DOS plateau, whereas for As21113—on an abrupt DOS slope, Fig. 5. Thus the hole doping will lead to a more significant growth of $N(E_F)$, which increases the probability of transition to magnetic state for As21113 rather than for P21113. For both phases electron doping will be accompanied by the lowering of $N(E_F)$ and will rapidly reduce the proximity to magnetism.

The obtained data allow us to estimate the Sommerfeld constants (γ) and the Pauli paramagnetic susceptibility (χ) for the examined phases under assumption of the free-electron model as $\gamma=(\pi^2/3)N(E_F)k_B^2$ and $\chi=\mu_B^2N(E_F)$. It is seen from Table III that both γ and χ decrease slightly when phosphorus is replaced by arsenic. On the other hand, the values of γ and χ obtained for P21113 and As21113 are comparable with those for other known FeAs and FeP SCs (Ref. 37)—for example, $\gamma\sim3.7$ mJ K^{-2} mol^{-1} for $LaFeAsO_{1-x}F_x$ and ~10 mJ K^{-2} mol^{-1} for LaFePO and ~10.8 mJ K^{-2} mol^{-1} for $BaNi_2As_2$.

D. Chemical bonding

To describe the interatomic bonding for the new phases P21113 and As21113, we begin with a simple ionic picture, which considers the standard oxidation numbers of atoms: Sr^{2+}, Sc^{3+}, Fe^{2+}, $(P,As)^{3-}$, and O^{2-}. Taking into account the distributions of atoms in the above-mentioned blocks of these crystals, their ionic formulas can be presented as $[(Fe^{2+})(P,As^{3-})]^{1-}[(Sr^{2+})_2(Sc^{3+})(O^{2-})_3]^{1+}$. Hence, the charge transfer occurs from positively charged blocks $[Sr_2ScO_3]^{\delta+}$ to negatively charged conducting blocks $[Fe(P,As)]^{\delta-}$ (like for other 1111, 122 and 111 FeAs and FeP superconductors, see Refs. 6, 7, 16, 32, 36, 38, and 39), and between these blocks the ionic bonding takes place. This picture is clearly visible in Fig. 6, where the charge-density map for P21113 is depicted. Besides, inside each block: $[Sr_2ScO_3]$ and [Fe(P,As)], the ionic bonding takes place between the ions with opposite charges: (Sr^{2+},Sc^{3+})-O^{2-} and Fe^{2+}-$(P,As)^{3-}$. Further, the charge-density distribution (Fig. 6) reveals also the mentioned covalent bonding Fe-P and Sc-O inside [FeP] and $[Sr_2ScO_3]$ blocks, respectively. It is very interesting that despite significant charge transfer from strontium atoms (see above), a certain overlapping of Sr orbitals with neighboring oxygen atoms occurs, which is indicative of partially covalent bonding of Sr ions. In addition, inside [Fe(P,As)] blocks the metalliclike Fe-Fe bonding occurs due to overlapping of the near-Fermi Fe 3*d* states. Thus, summarizing the above results, the intra-atomic bonding for P21113 and As21113 phases can be described as a high-anisotropic mixture of ionic, covalent, and metallic contributions.

IV. CONCLUSION

In summary, we have presented a detailed *ab initio* study of the structural and electronic properties of the newly synthesized tetragonal compounds $Sr_2ScFePO_3$ and $Sr_2ScFeAsO_3$ as prototype phases for the newly discovered family of 21113 systems, which offer new guidelines for the development of modern superconducting materials.

For both phases we obtain an almost similar band-structure picture around the Fermi level, where the Fermi level is crossed by low-dispersive quasi-two-dimensional-like bands, determined mainly by Fe 3*d* orbitals of [FeP] or [FeAs] blocks. The Fermi surfaces of $Sr_2ScFePO_3$ and $Sr_2ScFeAsO_3$ are also very similar to each other and to another FeAs and FeP SCs. Naturally, further theoretical and

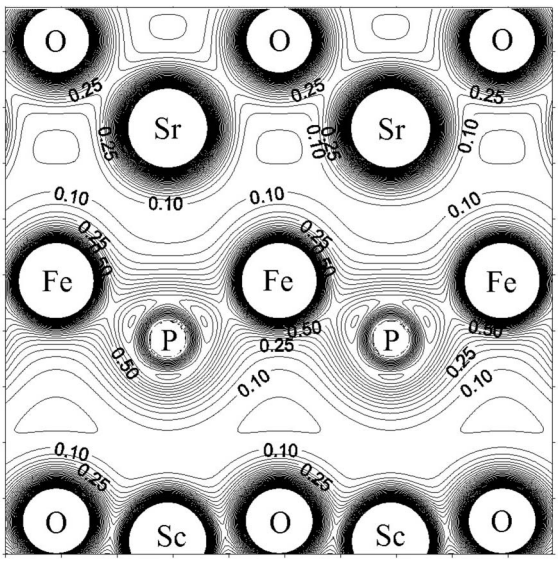

FIG. 6. Valence charge-density map (in $e/\mathrm{Å}^3$) for $Sr_2ScFePO_3$ in (100) plane.

experimental studies are necessary to clarify the details ofthe superconductivity mechanism for 21113 systems, as well as possible effects of hole or electron doping on the properties of these interesting materials.

ACKNOWLEDGMENTS

Financial support from the RFBR under Grant No. 09-03-00946-a is gratefully acknowledged.

*Corresponding author; shein@ihim.uran.ru

[1] Y. Kamihara, T. Watanabe, M. Hirano, and H. Hosono, J. Am. Chem. Soc. **130**, 3296 (2008).
[2] C. Wang, L. Li, S. Chi, Z. Zhu, Z. Ren, Y. Li, Y. Wang, X. Lin, Y. Luo, S. Jiang, X. Xu, G. Cao, and Z. Xu, EPL **83**, 67006 (2008).
[3] X. H. Chen, T. Wu, G. Wu, R. H. Liu, H. Chen, and D. F. Fang, Nature (London) **453**, 761 (2008).
[4] M. Rotter, M. Tegel, and D. Johrendt, Phys. Rev. Lett. **101**, 107006 (2008).
[5] H. Takahashi, K. Igawa, K. Arii, Y. Kamihara, M. Hirano, and H. Hosono, Nature (London) **453**, 376 (2008).
[6] A. L. Ivanovskii, Phys. Usp. **51**, 1229 (2008).
[7] M. V. Sadovskii, Phys. Usp. **51**, 1201 (2008).
[8] X. Zhu, F. Han, G. Mu, B. Zeng, P. Cheng, B. Shen, and H. H. Wen, Phys. Rev. B **79**, 024516 (2009).
[9] Z. A. Ren, W. Lu, J. Yang, W. Yi, X. L. Shen, Z. C. Li, G. C. Che, X. L. Dong, L. L. Sun, F. Zhou, and Z. X. Zhao, Chin. Phys. Lett. **25**, 2215 (2008).
[10] Y. Mizuguchi, F. Tomioka, S. Tsuda, T. Yamaguchi, and Y. Takano, Appl. Phys. Lett. **93**, 152505 (2008).
[11] Y. Kamihara, H. Hiramatsu, M. Hirano, R. Kawamura, H. Yanagi, T. Kamiya, and H. Hosono, J. Am. Chem. Soc. **128**, 10012 (2006).
[12] S. Lebègue, Phys. Rev. B **75**, 035110 (2007).
[13] T. Mine, H. Yanagi, T. Kamiya, Y. Kamihara, M. Hirano, and H. Hosono, Solid State Commun. **147**, 111 (2008).
[14] D. H. Lu, M. Yi, S. K. Mo, A. S. Erickson, J. Analytis, J. H. Chu, D. J. Singh, Z. Hussain, T. H. Geballe, I. R. Fisher, and Z. X. Shen, Nature (London) **455**, 81 (2008).
[15] T. M. McQueen, M. Regulacio, A. J. Williams, Q. Huang, J. W. Lynn, Y. S. Hor, D. V. West, M. A. Green, and R. J. Cava, Phys. Rev. B **78**, 024521 (2008).
[16] I. R. Shein and A. L. Ivanovskii, Phys. Rev. B **79**, 054510 (2009).
[17] Y. Kamihara, H. Hiramatsu, M. Hirano, H. Yanagi, T. Kamiya, and Y. Hosono, J. Phys. Chem. Solids **69**, 2916 (2008).
[18] A. I. Coldea, J. D. Fletcher, A. Carrington, J. G. Analytis, A. F. Bangura, J. H. Chu, A. S. Erickson, I. R. Fisher, N. E. Hussey, and R. D. McDonald, Phys. Rev. Lett. **101**, 216402 (2008).
[19] S. Lebègue, Z. P. Yin, and W. E. Pickett, New J. Phys. **11**, 025004 (2009).
[20] H. Ogino, Y. Katsura, S. Horii, K. Kishio, and J. Shimoyama, arXiv:0903.5124 (unpublished).
[21] G. F. Chen, T. L. Xia, P. Zheng, J. L. Luo, and N. L. Wang, arXiv:0903.5273 (unpublished).
[22] Y. L. Xie, R. H. Liu, T. Wu, G. Wu, Y. A. Song, D. Tan, X. F. Wang, H. Chen, J. J. Ying, Y. J. Yan, Q. J. Li, and X. H. Chen, arXiv:0903.5484 (unpublished).
[23] M. Tegel, F. Hummel, S. Lackner, I. Schellenbergb, R. Pöttgen, and D. Johrendt, arXiv:0904.0479 (unpublished).
[24] X. Zhu, F. Han, G. Mu, P. Cheng, B. Shen, B. Zeng, and H. H. Wen, arXiv:0904.1732 (unpublished).
[25] A. Pal, A. Vajpayee, R. S. Meena, H. Kishan, and V. P. S. Awana, arXiv:0904.3214 (unpublished).
[26] Y. Matsumura, H. Ogino, S. Horii, Y. Katsura, K. Kishio, and J. Shimoyama, arXiv:0904.0825 (unpublished).
[27] H. Ogino, Y. Matsumura, Y. Katsura, K. Ushiyama, S. Horii, K. Kishio, and J. Shimoyama, arXiv:0903.3314 (unpublished).
[28] X. Zhu, F. Han, G. Mu, P. Cheng, B. Shen, B. Zeng, and H. H. Wen, arXiv:0904.0972 (unpublished).
[29] P. Blaha, K. Schwarz, G. K. H. Madsen, D. Kvasnicka, and J. Luitz, *An Augmented Plane Wave Plus Local Orbitals Program for Calculating Crystal Properties* (Vienna University of Technology, Vienna, 2001).
[30] J. P. Perdew, K. Burke, and M. Ernzerhof, Phys. Rev. Lett. **77**, 3865 (1996).
[31] P. E. Blochl, O. Jepsen, and O. K. Andersen, Phys. Rev. B **49**, 16223 (1994).
[32] I. R. Shein, V. L. Kozhevnikov, and A. L. Ivanovskii, Phys. Rev. B **78**, 104519 (2008).
[33] C. H. Lee, H. Eisaki, H. Kito, M. T. Fernandez-Diaz, T. Ito, K. Kihou, H. Matsushita, M. Braden, and K. Yamada, J. Phys. Soc. Jpn. **77**, 083704 (2008).
[34] V. Vildosola, L. Pourovskii, R. Arita, S. Biermann, and A. Georges, Phys. Rev. B **78**, 064518 (2008).
[35] D. J. Singh and M. H. Du, Phys. Rev. Lett. **100**, 237003 (2008).
[36] I. R. Shein and A. L. Ivanovskii, JETP Lett. **89**, 41 (2009).
[37] P. J. Baker, S. R. Giblin, F. L. Pratt, R. H. Liu, G. Wu, X. H. Chen, M. J. Pitcher, D. R. Parker, S. J. Clarke, and S. J. Blundell, New J. Phys. **11**, 025010 (2009).
[38] I. R. Shein and A. L. Ivanovskii, Scr. Mater. **59**, 1099 (2008).
[39] I. R. Shein and A. L. Ivanovskii, JETP Lett. **88**, 683 (2008).